

## SUPPLEMENTARY FIGURES TABLE OF CONTENTS

**Supplementary Figure 1.** Female AVF blood flow rate and body weight compared to age-matched male animals.

**Supplementary Figure 2.** *In vivo* imaging and blood flow measurement study protocol.

**Supplementary Figure 3.** Representative histological images of AVF outflow using H&E and Carstairs' staining.

**Supplementary Figure 4.** Morphological assessments of AVF using Carstairs' and Picrosirius red staining.

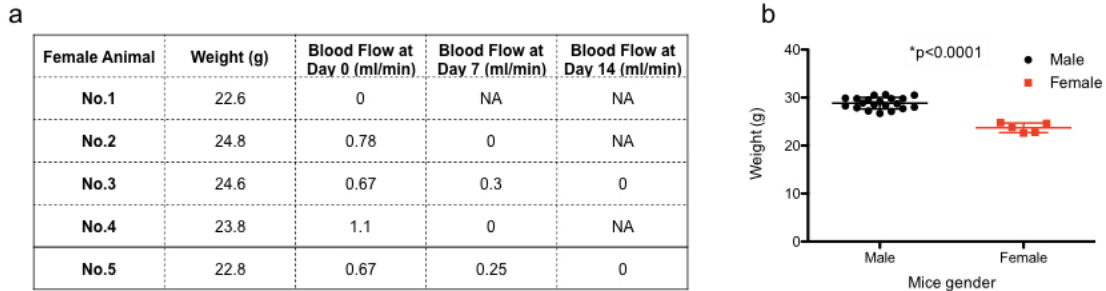
**Supplementary Figure 5.** Histological analyses of AVF outflow and collagen content.

**Supplementary Figure 6.** Representative intravital microscopy (IVM) imaging of fibrin (FTP11) and macrophage content (CLIO-VT680) in arteriovenous fistulas (AVFs) and contralateral control jugular veins.

**Supplementary Figure 7.** *In vivo* AVF blood flow rate measurements and Kaplan-Meier survival analysis of fistula patency using a range of blood flow rates to define fistula occlusion.

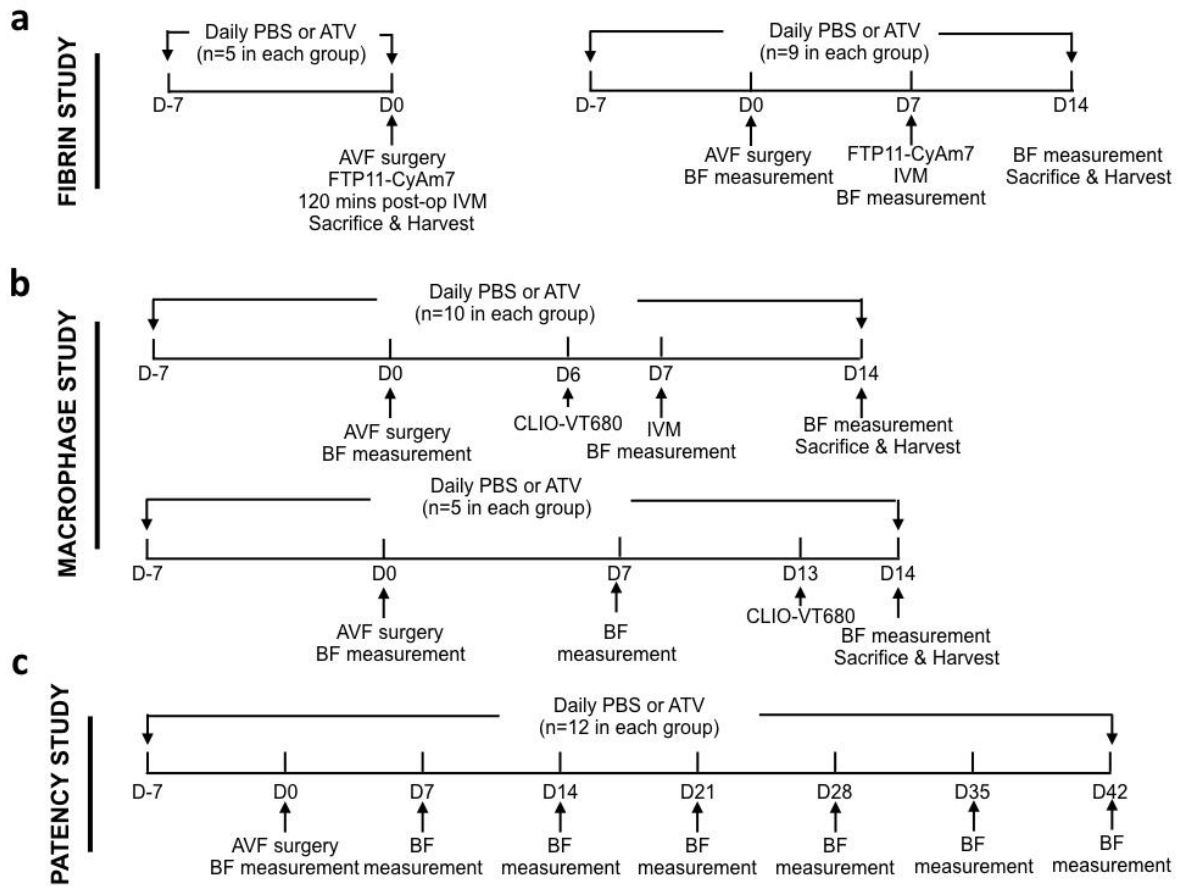
## SUPPLEMENTARY FIGURES

### Supplementary Figure 1



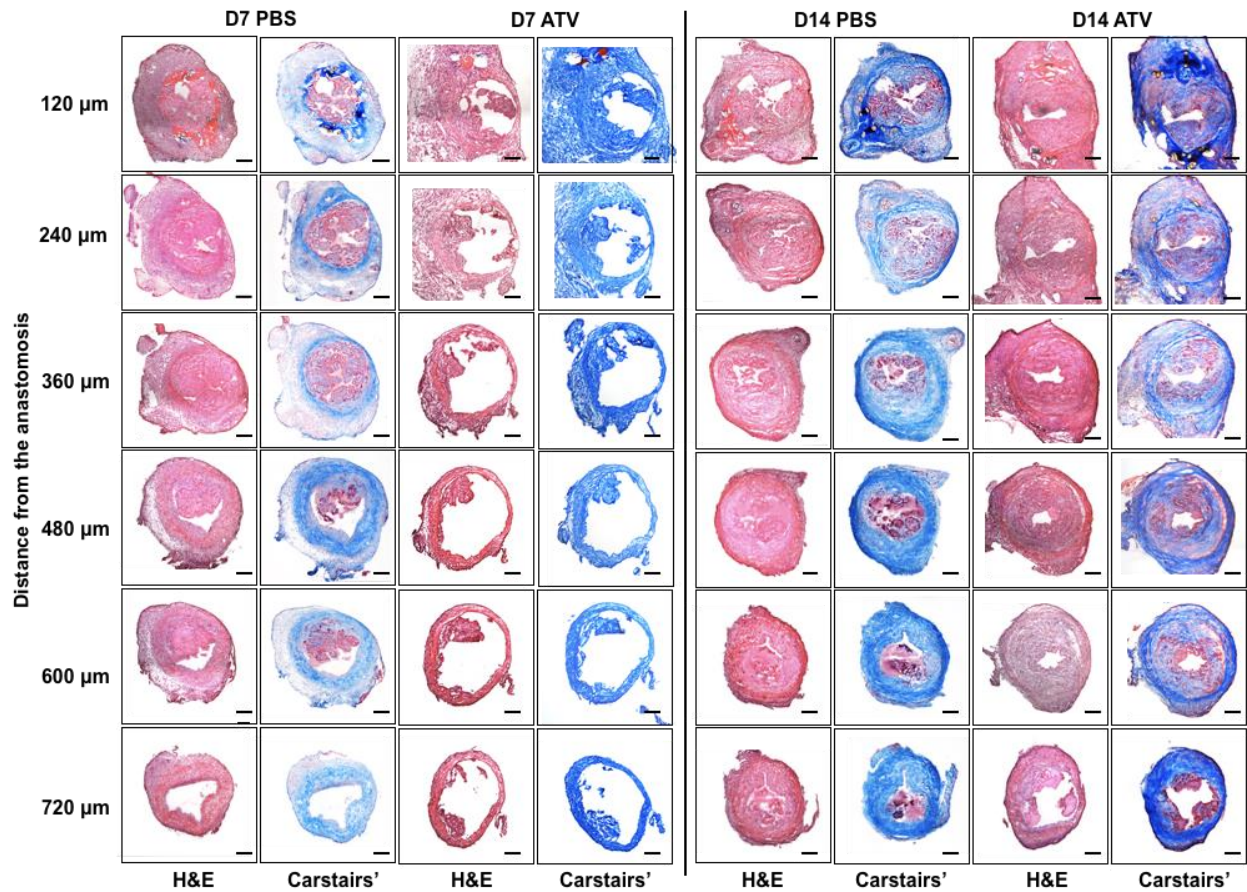
**Supplementary Figure 1.** Female AVF blood flow rate and body weights compared to age-matched male mice. a. AVFs were created in female animals (n=5) using the same surgical protocol as in males. One female AVF was occluded immediately post-operatively. Two fistulas were found to be occluded on day 7. The remaining two fistulas were found to be occluded on day 14. b. The body weight of female mice was significantly lower than that of age-matched female mice ( $p < 0.0001$ ).

## Supplementary Figure 2



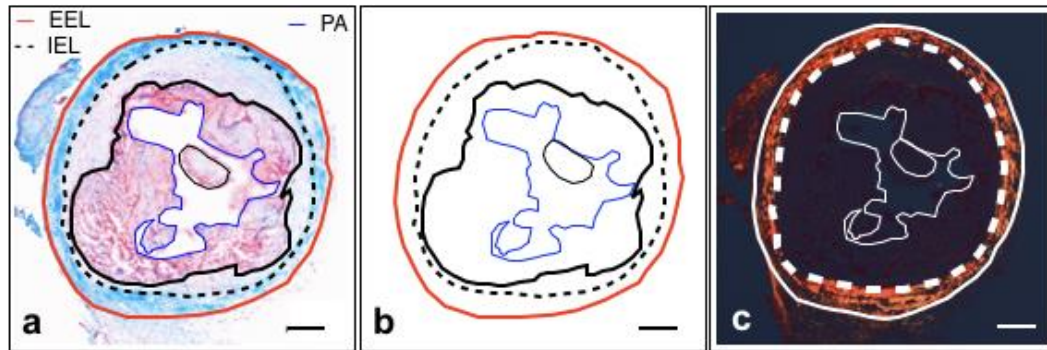
Supplementary Figure 2. *In vivo* imaging and blood flow measurement study protocol.

### Supplementary Figure 3



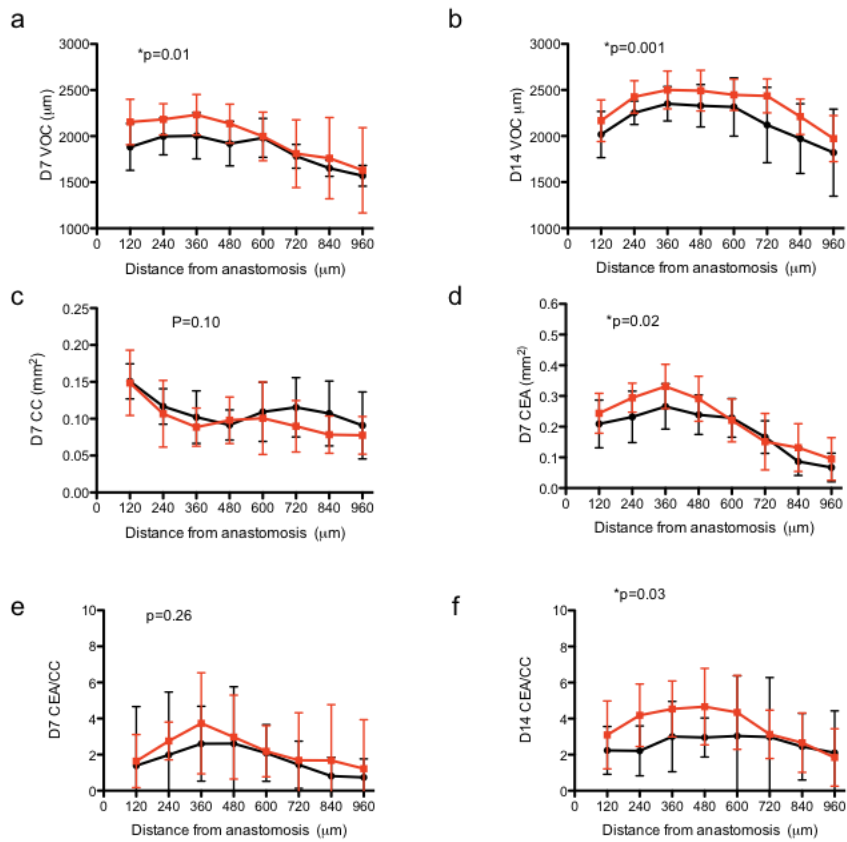
**Supplementary Figure 3.** Representative histological images of AVF outflow using H&E and Carstairs' staining. AVF tissue sections were stained every 120μm with hematoxylin and eosin (H&E) to assess general morphology, and Carstairs' stain to identify collagen, fibrin and neointimal hyperplasia. Scale bar: 100 μm.

## Supplementary Figure 4



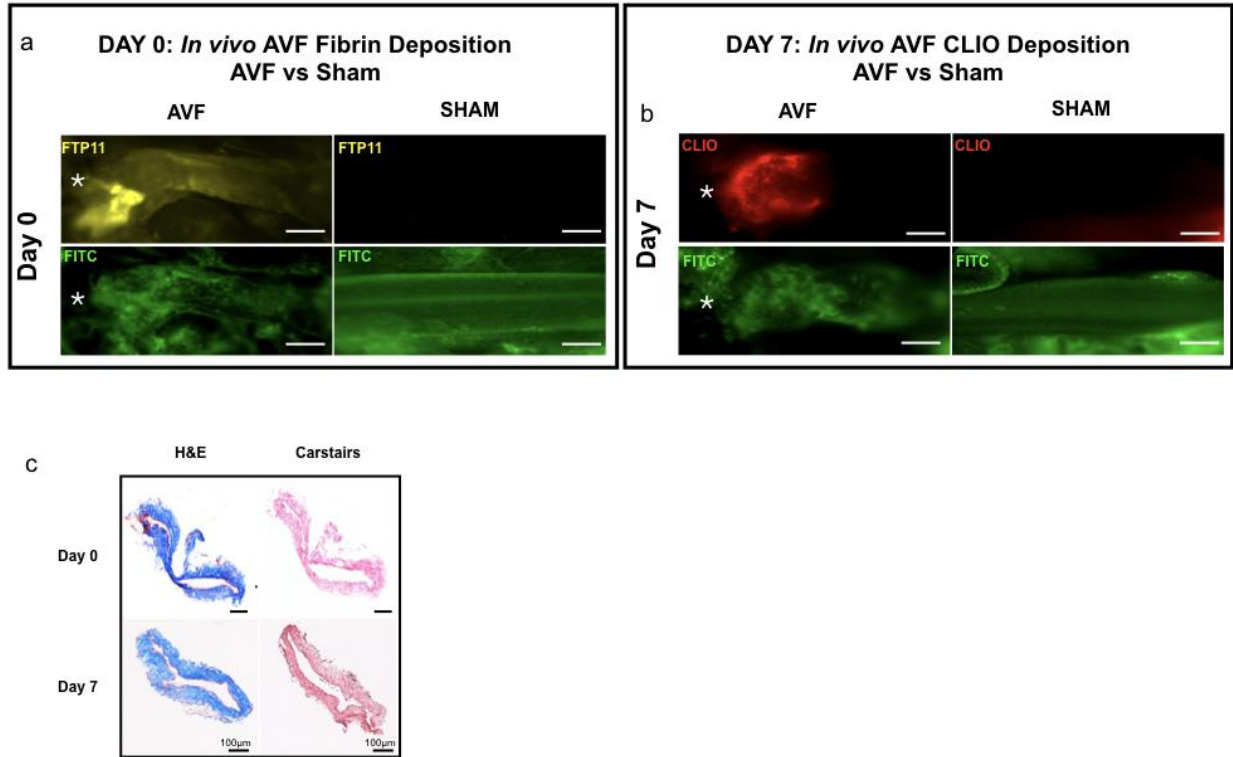
**Supplementary Figure 4.** Morphological assessments of AVF using Carstairs' and Picrosirius red staining. **a.** Venous outflow area, neointimal hyperplasia area, thrombus burden and patent area were all measured and calculated using Carstairs' staining. Red line: EEL (external elastin lamina); Dashed line: IEL (internal elastin lamina); Thick solid black line: neointimal hyperplasia border; Blue line: Patent Area (PA, defined as the area within the inner blue solid line). **b.** Schematic figure. NH area: area between dash line and thick solid black line. Thrombus area: area between thick solid black line and thin blue line. Patent area: area enclosed by the thin blue line. **c.** Picrosirius red staining was used to measure collagen content. Solid white line: outside border of collagen content. Dashed white line: inside border of collagen content. Scale bar: 100  $\mu\text{m}$ .

## Supplementary Figure 5



**Supplementary Figure 5.** Histological analyses of AVF outflow limb. **a,b:** Carstairs' histological analysis showed atorvastatin (ATV) increased the outer circumference of the AVF venous outflow limb at both day 7 and day 14 ( $p < 0.05$ ). **c:** Picrosirius red staining analysis showed that the day 7 collagen content was comparable in PBS and ATV-treated group ( $p=0.10$ ). **d:** The collagen-enclosed area, defined as the AVF area within the outer border defined by PSR staining, was also larger in the atorvastatin-treated group on day 7 ( $p = 0.02$ ). **e,f:** The ratio of collagen-enclosed area to collagen content, a measure of favorable AVF remodeling, was similar between groups at day 7 ( $p = 0.26$ ) but was significantly higher in ATV-treated animals by day 14 ( $p = 0.03$ ). VOC: vein outer circumference; CC: collagen content; CEA: collagen enclosed area.

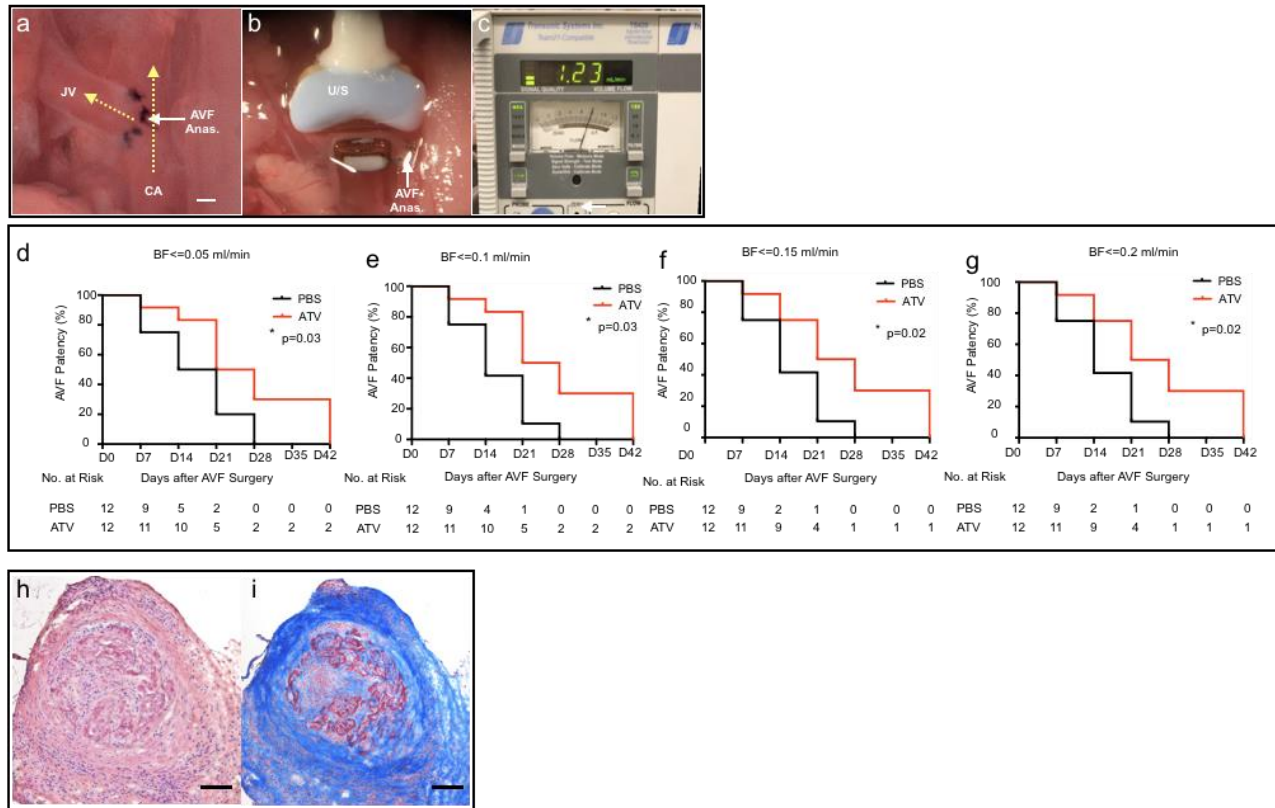
## Supplementary Figure 6



**Supplementary Figure 6.** Representative intravital microscopy (IVM) imaging of fibrin (FTP11) and macrophage content (CLIO-VT680) in arteriovenous fistulas (AVFs) and contralateral control jugular veins. **a.** The signal intensity of FTP11-CyAm7 at day 0 was significantly higher in AVFs compared to the contralateral control jugular vein; Scale bar: 250 $\mu$ m. **b.** The signal intensity of CLIO-VT680 at day 7 was significantly higher in AVFs compared to the contralateral sham-operated control jugular vein; Scale bar: 250 $\mu$ m. **c.** Representative hematoxylin and eosin histological staining of contralateral sham-operated jugular veins at day 0 and day 7 showed a thinner vein wall compared to the AVF vein wall.



## Supplementary Figure 7



**Supplementary Figure 7.** Murine AVF blood flow was measured by Transonic flow probe. **a.** Murine AVF was created using an end-to-side jugular vein and carotid artery anastomosis. CA: Carotid artery; JV: Jugular vein; White arrow: AVF juxta-anastomosis; Yellow arrow: the direction of AVF blood flow. Scale bar: 500 $\mu$ m. **b.** AVF blood flow was measured using a blood flow probe *in vivo*. **c.** In this mouse, the AVF blood flow was measured as 1.23 ml/min using the flow probe. **d-g.** Kaplan-Meier survival analysis of fistula patency using a range of blood flow rates to define fistula occlusion. At each blood flow rate, atorvastatin prolonged arteriovenous fistula patency (0.05-0.20 mL/min, all  $p < 0.05$ ). **h-i.** Representative pathology of occluded AVF at day 28-42. H&E and Carstairs' staining of day 28 thrombosed AVF shows a fistula lumen was occluded by neointimal hyperplasia and thrombus. Scale bar: 100 $\mu$ m.